

# Aerodynamic impact of total inferior turbinectomy versus inferior turbinoplasty – a computational fluid dynamics study\*

Joey Siu<sup>1</sup>, Kiao Inthavong<sup>2</sup>, Yidan Shang<sup>2</sup>, Sara Vahaji<sup>3</sup>, Richard George Douglas<sup>1</sup>

**Rhinology** 58: 4, 349- 359, 2020  
<https://doi.org/10.4193/Rhin20.011>

<sup>1</sup> Department of Surgery, The University of Auckland, Auckland, New Zealand

<sup>2</sup> Mechanical & Automotive Engineering, School of Engineering, RMIT University, Bundoora, Victoria, Australia

<sup>3</sup> School of Engineering, Deakin University, Waurn Ponds, Victoria, Australia

**\*Received for publication:**

January 8, 2020

**Accepted:** February 24, 2020

## Abstract

**Background:** The aim of this study was to investigate using computational fluid dynamics (CFD) the effects on nasal aerodynamics of two different techniques for reducing the inferior turbinate. This may assist in surgical planning to select the optimal procedure.

**Methods:** Virtual surgery using two techniques of turbinate reduction was performed in eight nasal airway obstruction patients. Three bilateral nasal airway models for each patient were compared: 1) Pre-operative 2) Bilateral inferior turbinoplasty 3) Bilateral total inferior turbinate resection (ITR). Two representative healthy models were included. CFD modeling of airflow was performed under steady-state, laminar, inspiratory conditions.

**Results:** Nasal airway resistance was slightly more reduced following ITR compared to turbinoplasty due to loss of the pressure gradient at the head of the IT. Turbinoplasty resulted in ventilation, pressure and wall shear stress profiles closer to those of healthy models. A more prominent jet-like course of the main flow stream was observed inferiorly in the ITR group.

**Conclusions:** Nasal air conditioning was significantly altered following IT surgery. Overall differences between the groups were small and are unlikely to bear influence on nasal function in normal environments. Further studies using a larger number of patients and healthy subjects are required, attempting to establish a clinical correlation with long-term outcomes such as the perception of nasal patency, mucosal crusting and drying, and air conditioning in different environments. Since a large proportion of IT mucosa remains following turbinoplasty, future dependence on topical therapy should also be considered.

**Key words:** computational fluid dynamics, computer simulation, nasal airflow, nasal cavity, nasal obstruction, turbinate, rhinitis

## Introduction

Inferior turbinate enlargement and resultant nasal airway obstruction (NAO) can be treated by a range of techniques<sup>(1)</sup>. Preserving most of the turbinate mucosa is believed to help maintain the normal physiology of the mucosa<sup>(1-3)</sup>. Currently, there are very few prospective clinical trials comparing different techniques for inferior turbinate surgery, assessing long-term results and complications<sup>(1,4,5)</sup>. These studies tend to have heterogeneous cohorts and few of them use objective measures such as acoustic rhinometry and rhinomanometry. Objective

methods of assessment of nasal patency are not routinely utilized in clinical practice to select suitable patients for surgery as it has been found that there is a poor correlation between objective measures and subjective appreciation of nasal patency<sup>(6)</sup>. Computational fluid dynamics (CFD) techniques have been used in some studies to model the effects of inferior turbinate enlargement and inferior turbinate surgery but these have not yet provided a consensus about which is the best procedure<sup>(7-11)</sup>. Confounding factors including the extent of surgery, as well as the presence of a concomitant septal deviation<sup>(8-10)</sup>.

Virtual surgery allows prediction of post-operative changes in aerodynamics by computer simulations<sup>(7-10)</sup>. These changes may impact on surgical outcomes and contribute to complications such as persistent nasal obstruction, hyposmia, mucosal drying and crusting<sup>(12,13)</sup>. Although total inferior turbinate resection (ITR) often leads to a significant drop in nasal resistance compared to more conservative turbinate reduction methods, it has been suggested that this procedure may lead to disrupted flow patterns associated with reduced subjective nasal patency and air-conditioning capacity<sup>(7-10,12,14)</sup>.

This is the largest computational study to date evaluating the effects of different extents of bilateral inferior turbinate reduction on airflow changes and air-mucosal interactions in eight NAO patients undergoing surgery. Virtual models of turbinoplasty by resection of the lower bulk of the inferior turbinate and ITR were compared with pre-operative NAO and healthy models.

## Materials and Methods

### Subjects

Eight patients with nasal obstruction undergoing surgery (inferior turbinate surgery with or without septoplasty) for turbinate hypertrophy resistant to medical treatment were selected for the study (Table 1). These patients had no evidence of sinusitis on clinical assessment or CT. Only patients with minor septal deviation or no septal deviation on endoscopic and radiologic assessment were included. Three-dimensional reconstructions of the nasal passages including paranasal sinuses were created from pre-operative CT scans. Representative healthy nasal models were constructed from two normal subjects without any sino-nasal complaints (Table 1). Nasal cavity mucosal health was confirmed with endoscopy. Reconstruction of nasal models was performed from MRI images for healthy subject A and CT

images for healthy subject B. The MRI scan was performed according to a high-resolution MRI protocol<sup>(15)</sup>. The combination of parameters was sufficient to distinguish the air and soft tissue interface for the segmentation of the sinuses and ostia. Healthy subject B had a history of Grave's ophthalmopathy requiring orbital decompression and underwent CT imaging as part of the pre-operative work up. None of the study subjects received nasal decongestant prior to their scans or endoscopic assessments to ensure the closest correlation between clinical and radiological assessment and to reflect the most common state of breathing that patients experience in daily life. Written informed consent was obtained from all patients.

### CFD sinonasal model reconstruction

All scans were imported into a medical imaging software package, 3D Slicer<sup>®</sup>. After airway segmentation and smoothing and correction for artefacts, a three-dimensional surface geometry of each subject's sinonasal airways including the outer nose and face was created. A virtual septoplasty was performed using 3D Slicer<sup>®</sup> in three patients who underwent septoplasty (Table 1) in addition to inferior turbinate surgery. Therefore, all reconstructed pre-operative nasal models in this study had inferior turbinate hypertrophy without septal deviation. The reconstructed nasal models were then exported from 3D Slicer<sup>®</sup> in stereolithography (STL) file format into the CAD software package Geomagic Wrap<sup>®</sup> for further processing to extract the sinonasal cavity geometry and separate it into regions for investigating particle deposition. Each sinonasal cavity was separated into the following regions (Figure 1): vestibule (anterior to internal nasal valve), inferior nasal cavity (below superior border of inferior turbinate), middle nasal cavity (from superior border of inferior turbinate below to superior border of middle turbinate above),

Table 1. Subject demographics and surgical intervention.

Subject	Ethnicity	Gender	Age	Previous surgery	Septum deviation	Surgery	% volume reduction after virtual turbinoplasty (R, L)	% surface area reduction after virtual turbinoplasty (R, L)
1	NZ European	F	58	None	None	Turbinate	47, 58	28, 31
2	NZ European	F	55	None	None	Turbinate	44, 66	22, 40
3	Israeli	M	44	FESS	None	Turbinate	51, 37	21, 12
4	Chinese	M	30	None	Mild caudal	Septum, turbinate	34, 32	11, 19
5	NZ European	F	49	None	None	Turbinate	37, 38	22, 28
6	NZ European	M	17	None	None	Turbinate	36, 48	15, 20
7	NZ European	F	61	None	Mild caudal	Septum, turbinate	52, 67	25, 37
8	NZ European	F	53	None	Mild right-sided	Septum, turbinate	52, 45	24, 22
9 (Healthy A)	Chinese	F	26	None	None	None	N/A	N/A
10 (Healthy B)	NZ European	F	65	None	None	None	N/A	N/A

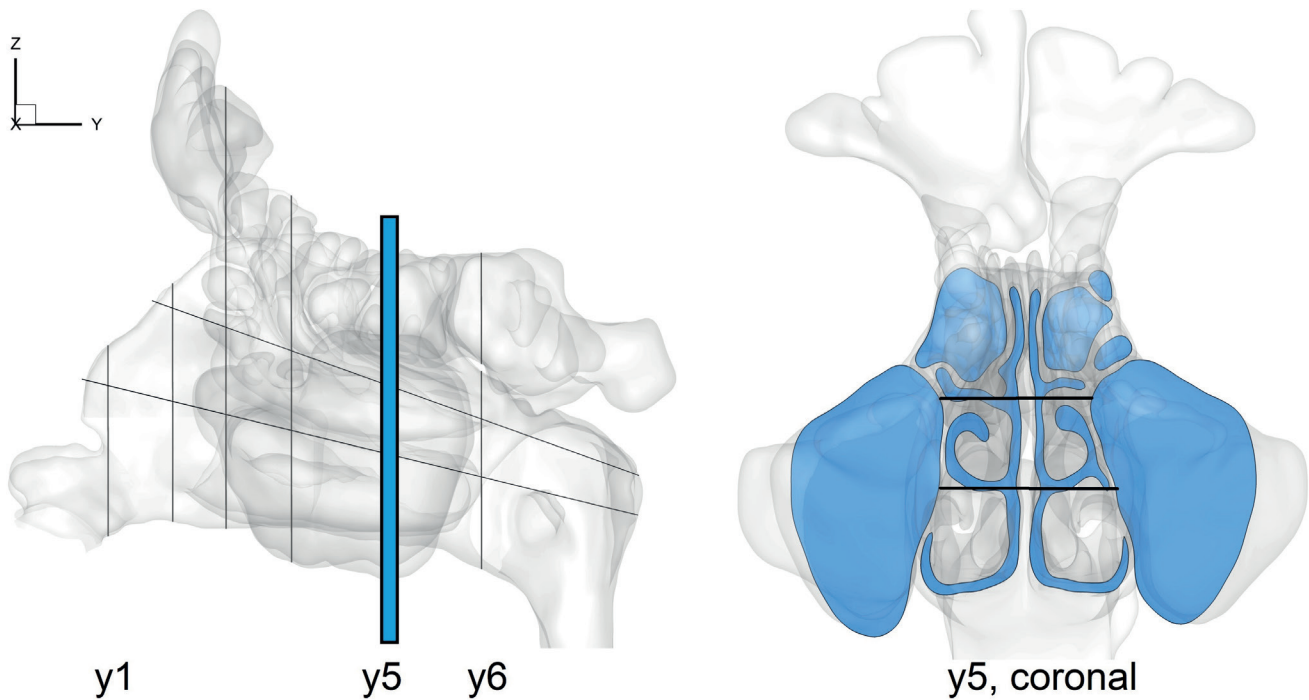


Figure 1. Sinonasal cavity geometry with coronal sections along the mainstream and transverse partitions separating superior, middle and inferior nasal cavity (left), coronal section y5 with partitions separating superior, middle and inferior nasal cavity (right).

superior nasal cavity (olfactory cleft, above superior border of middle turbinate), maxillary sinus and nasopharynx.

#### Creation of virtual inferior turbinate surgery models

Two different methods of inferior turbinate surgery were performed for all eight patients using Geomagic Wrap®: i) turbinoplasty by resection of the lower bulk (one third to one half of the inferior turbinate) ii) total inferior turbinectomy. Accounting for the 8 preoperative patient models, 16 virtual surgery models (Figure 2) and 2 healthy models, a total of 26 different nasal cavity models were investigated.

#### CFD Modelling

The 3D model was meshed with polyhedral cells with prism layers using ANSYS-Fluent 2019R1. The mesh quality was improved by moving nodes so that the maximum skewness in all models were less than 0.65. A mesh independence test was performed by comparing the velocity magnitude on six 2D-cross-sectional planes<sup>16</sup> and found optimised mesh between 1.5-2.2 million polyhedral and prism cells for all models. A steady inhalation flow rate of 15 L/min was used and a laminar flow model was applied.

#### Numerical analysis

The distribution of ventilation and wall shear stress in each nasal cavity partition (superior, middle and inferior, Figure 1) was evaluated from their average respective values in the mainstream through coronal slices y3, 4 and 5. Nasal resistance is the ratio

between pressure change from nostril to nasopharynx and total flow rate. Pressure distribution was evaluated using pressure contours and by calculating pressure variations from the nostril to the nasopharynx outlet including coronal slices y1-6 (Figure 1). All statistical analyses were performed using Microsoft Excel (Microsoft Corporation, Washington). The student's T test was applied to analyse differences in total pressure drop, ventilation and wall shear stress values between the pre-operative, turbinoplasty and ITR groups.

#### Results

Following virtual turbinoplasty, patients had a mean inferior turbinate volume reduction of 47% (range 34-66%) and mean surface area reduction of 24% (range 11-40%). Individual percentage volume reduction and surface area reduction for each model is shown in Table 1.

#### Streamline plots and velocity contours

Representative streamline plots and velocity contours are shown in Figures 3 and 4, respectively, for patient 5 (preoperative, turbinoplasty and ITR) and healthy subject B. Despite differences in nasal valve geometry and surgery there was no significant difference in average velocity at the nasal valve between the three groups. Between the nasal valve and the head of the inferior turbinate, airflow velocity increased with the extent of turbinate surgery (slice y2, Figure 4).

In healthy subjects, the streamlines mostly traversed the common meatus adjacent to the inferior and middle turbinate at a

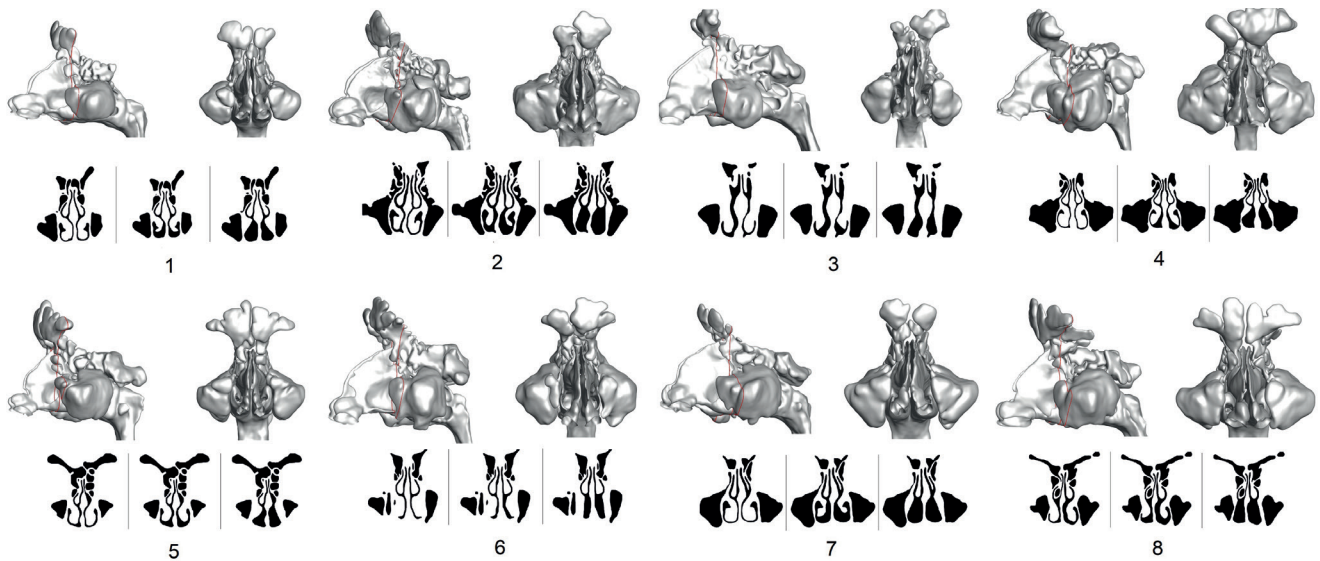


Figure 2. 3D nasal cavity geometry for subjects 1-8 in the study with accompanying selected coronal section; pre-operative (left), turbinoplasty (middle), turbinectomy (right).

moderate velocity (Figure 3d). But the streamlines were relatively uniformly distributed and reached the superior nasal cavity including the olfactory cleft. In the preoperative group, the flow stream was pushed by the bulk of the inferior turbinates slightly more superiorly, moving faster in the middle nasal passage adjacent to the middle turbinate, with lower velocity streamlines reaching the superior nasal cavity including the olfactory cleft (Figure 3a, 4a). The middle meatus space received higher airflow in the healthy group compared to the preoperative group (slices y3-5, Figure 4d). Vortices in obstructed patients were common in the anterior dorsal region and bend of the nasopharynx. They were also found in the ethmoidal air cells and around the maxillary ostia in some patients.

Following any turbinate surgery, flow became more concentrated inferiorly and was more jet like (Figures 3b-c, 4b-c). In the turbinoplasty group, the distribution of the flow stream was closer to that of a healthy subject, as the main flow route was through the common meatus adjacent to the middle and inferior turbinates (Figure 4b). However, flow velocity was faster. Despite air moving faster in the turbinoplasty models, ventilation of the middle meatuses did not improve as the jet flow sheared against the medial surfaces of the middle and inferior turbinates and medial nasal floor, with very little distribution of streamlines laterally (Figure 3b, 4b). When they occurred, they appeared to be more prominent. For the ITR group, airflow was even more concentrated and jet-like compared to the turbinoplasty group, with a high peak velocity in the region on the infero-medial surface of the middle turbinate (Figure 3c, 4c). Airflow does not appear to take up the space created by removing the entire inferior turbinate (Figure 4c). There were many fewer streamlines moving along the nasal floor or superiorly

compared to the healthy, preoperative and turbinoplasty groups (Figure 3c). Although the main flow stream was the level of the middle turbinate, due its increased jet-like behaviour compared with other groups, it had reduced contact with the septum and lateral wall and streamlines did not have the opportunity to travel into the middle meatus (Figure 3c, 4c; slices y3-5). Vortices in the inferior nasal cavity were common in both surgery groups. While patient 3 (post-FESS) had a greater density of streamlines in the middle meatus and in proximity to the maxillary ostium compared to other patients, very slow airflow entered the sinuses in any of the preoperative or surgery models. No other obvious differences were observed for this patient.

#### Flow partitioning

Flow partitioning results in the three regions (superior, middle and inferior nasal cavities) are displayed in Table 2 and Figure 5a. Ventilation in the inferior nasal cavity was higher in the surgery groups compared to the preoperative group (turbinoplasty  $p=0.04$ , ITR  $p=0.001$ ). There was no significant difference in airflow in the middle nasal cavity and superior nasal cavity between the groups. However, compared to the turbinectomy group, the ventilation profile for the turbinoplasty group reflected more closely that of the healthy group (Figure 5a).

#### Pressure distribution

Figure 6 shows a comparison of pressure contours for patient 5 (preoperative, turbinoplasty and ITR) and healthy subject B. Figure 7 shows pressure variations from the nostril to nasopharynx outlet for each group. There was a large difference in total pressure drop between the preoperative group and both surgery groups ( $p<0.0001$ ) but there was only a small difference

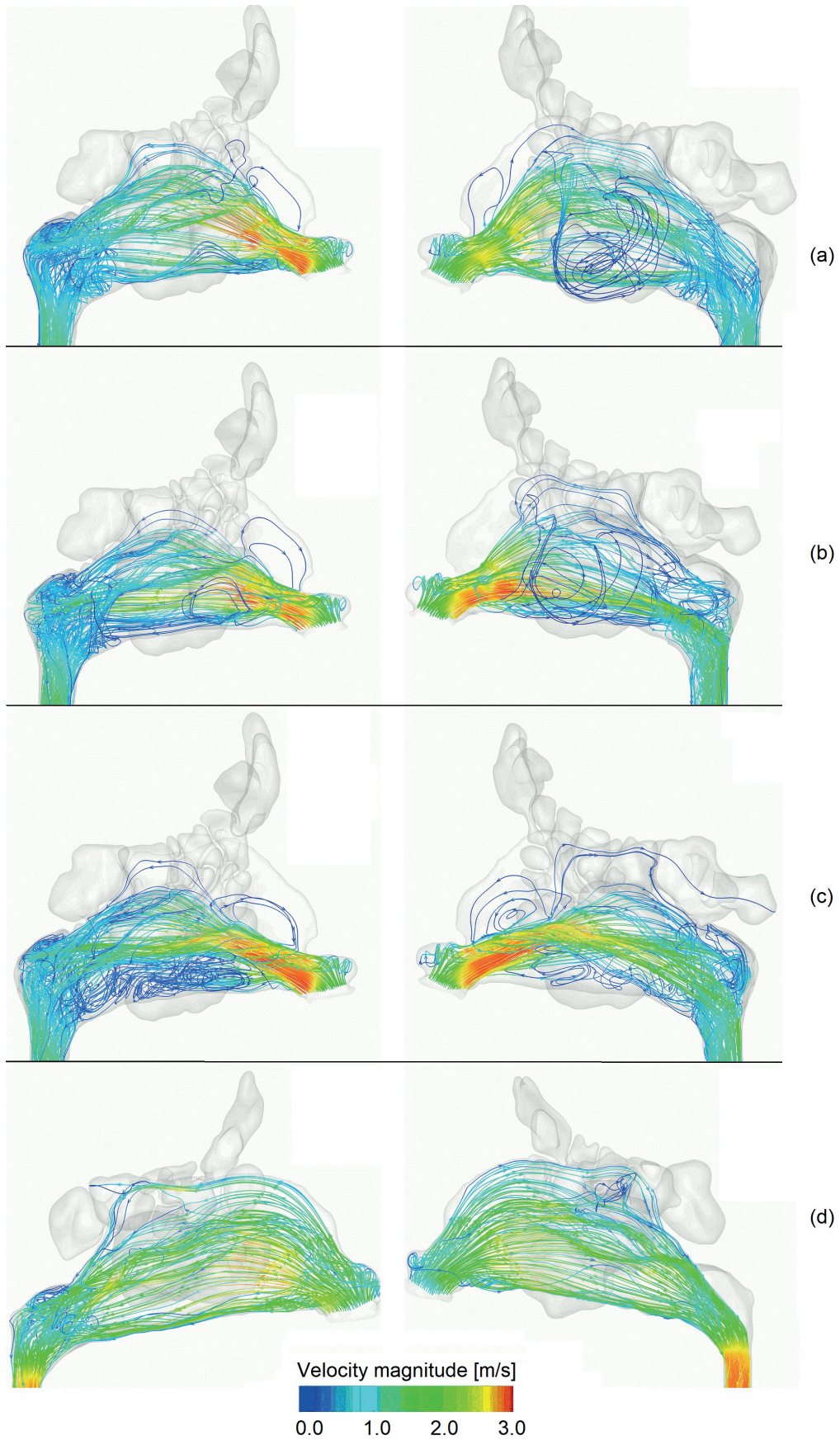


Figure 3. Streamline plots; right sinusal cavity (left), left sinusal cavity (right). (a) Preoperative (b) Turbinoplasty (c) Turbinectomy (d) Healthy subject B.

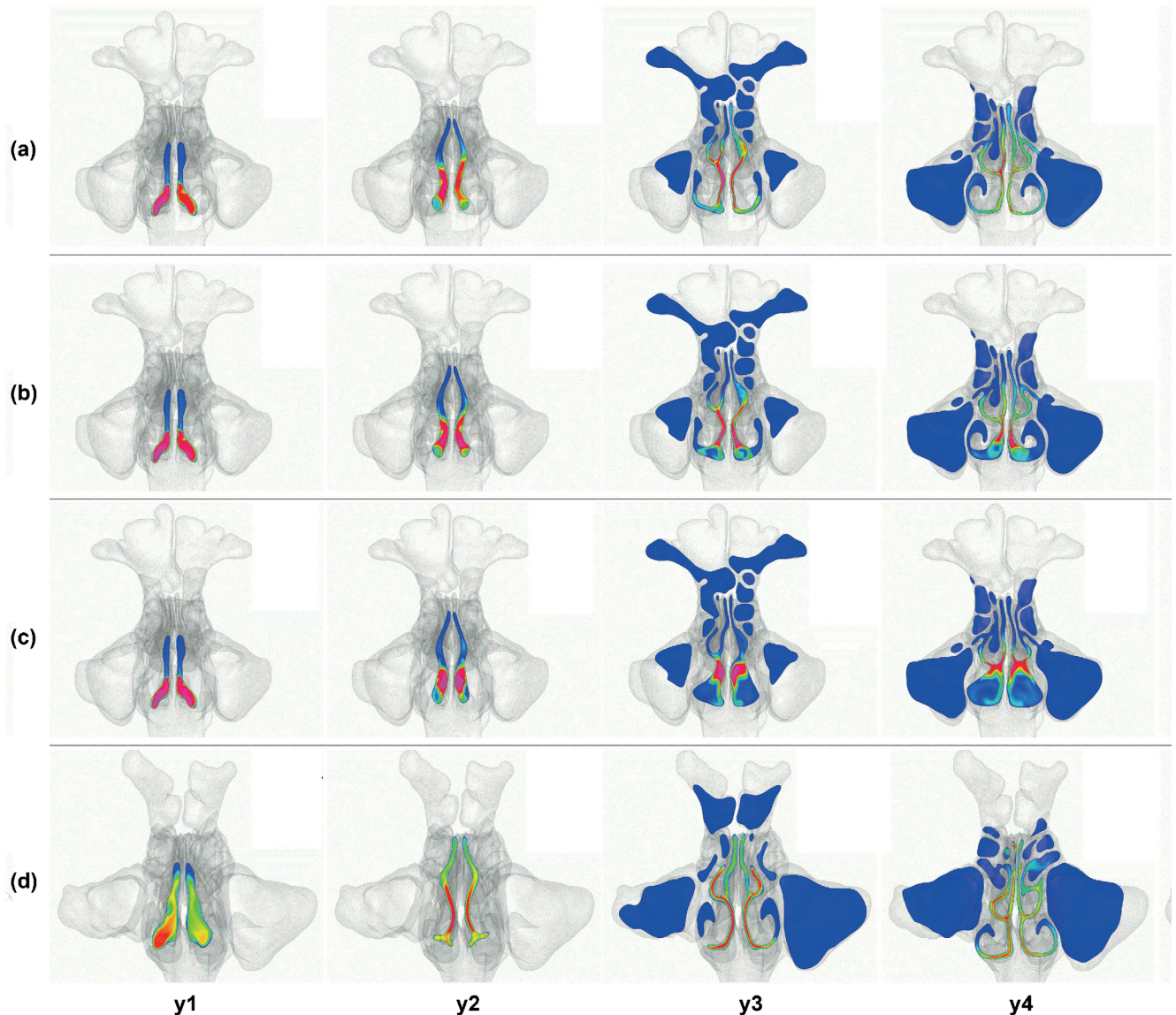


Figure 4. (Left) Velocity contours (a) Preoperative (b) Turbinoplasty (c) Turbinectomy (d) Healthy subject B.

in mean total pressure drop of 1.3Pa between the turbinoplasty and ITR group ( $p=0.002$ ). In all preoperative models, there was a large initial pressure gradient at the head of the inferior and middle turbinates (Figure 6a). In addition, there was often an additional large gradient at the nasal valve. Large gradations in pressure occurred towards nasopharynx. In healthy subjects, similar locations of pressure gradients were seen but there was a smoother pressure drop and pressures were lower (Figure 6d). The majority of turbinoplasty and ITR models had a single major initial pressure drop in the nasal valve, involving a smaller zone of high pressure compared with the preoperative group (Figure 6b, c). The pressure gradient at the head of the inferior turbinate tended to be diminished compared to the preoperative group in both groups (Figure 6b, c and 7). This difference was statistically significant in the ITR group ( $p=0.04$ ) but not the turbinoplasty

group. Throughout the rest of the nasal cavity posteriorly, turbinoplasty models had a similar pressure variation compared with the healthy subjects, but pressures were lower and more uniform through the nasal cavity (Figure 6c). The ITR group had the most uniform pressure in the nasal cavity before dropping at the nasopharynx (Figure 6d).

#### Wall shear stress

WSS distribution was analysed as a measure of air-mucosa contact in three regions (superior, middle and inferior nasal cavities). Results are displayed in Table 2 and Figure 5b. WSS was lower in the superior nasal cavity for the ITR group compared to the turbinoplasty group ( $p=0.0002$ ) but not compared to the preoperative group ( $p=0.06$ ). WSS was lower in the middle nasal cavity for the ITR group compared to both the preoperative

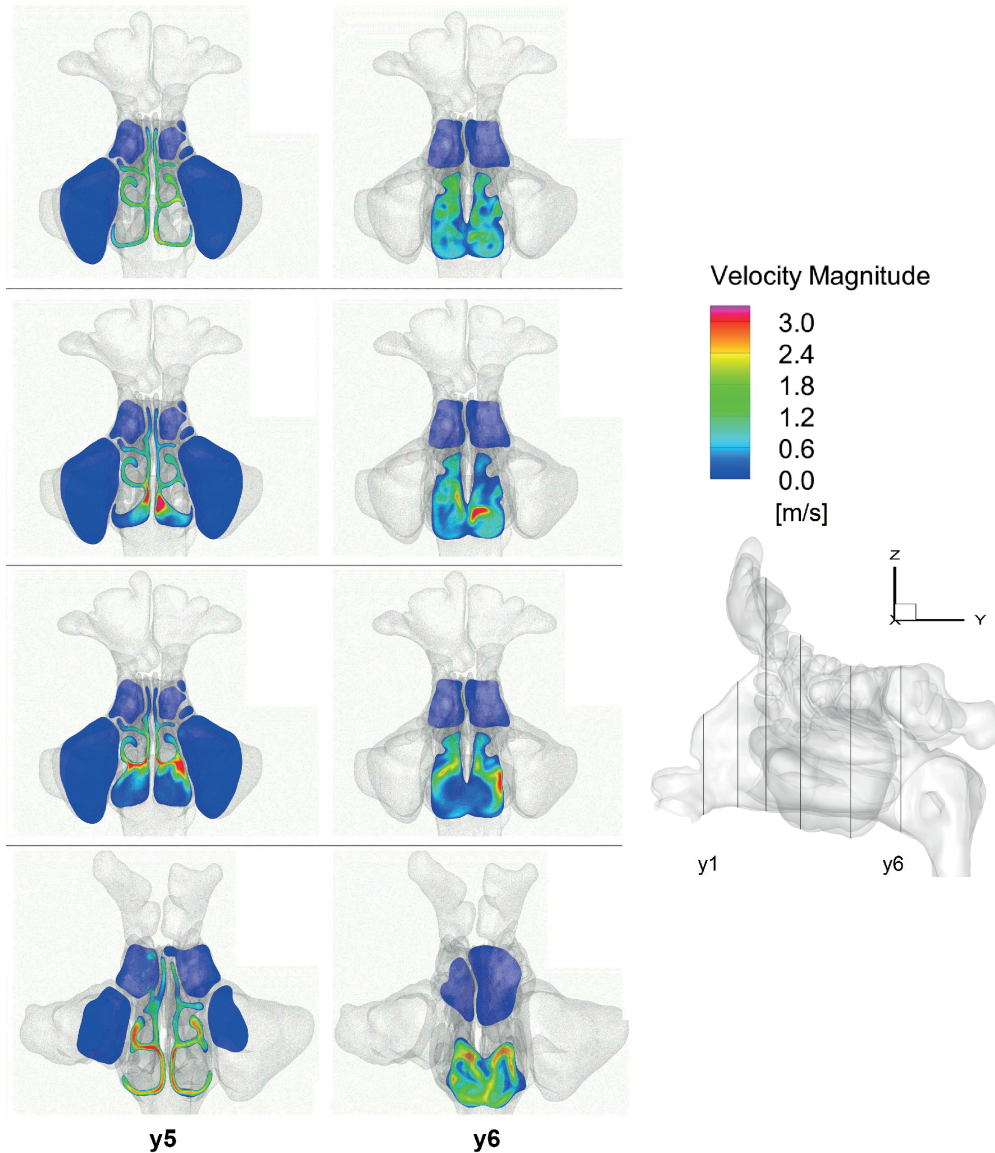


Figure 4. (Right) Velocity contours (a) Preoperative (b) Turbinoplasty (c) Turbinectomy (d) Healthy subject B.

group ( $p=0.03$ ) and the turbinoplasty group ( $p=0.04$ ). WSS was lower in the inferior nasal cavity for the ITR group compared to the preoperative group ( $p=0.04$ ) but not the turbinoplasty group ( $p=0.65$ ). There was no significant difference in WSS in the superior, middle or inferior nasal cavities between the preoperative and turbinoplasty groups. Compared to the ITR group, the wall shear stress profile for the turbinoplasty group was more similar to that of the healthy group (Figure 5b).

## Discussion

This is the largest computational study to date comparing two techniques of inferior turbinate surgery performed virtually in eight patients with nasal airway obstruction secondary to inferior turbinate hypertrophy. Three bilateral nasal airway models for each patient were compared and two representative healthy

models were also analysed for comparison. A small number of CFD studies have evaluated aerodynamics, humidification, and warming following inferior turbinate resection<sup>(7,9,10,12,17-21)</sup>. The majority of them have included healthy subjects for virtual surgery, frequently studying them as single-pilot subjects, and/or unilateral models, limiting interpretation of the results and generalization for nasal obstruction patients requiring bilateral inferior turbinate surgery. The relationship of the inferior turbinate within the nasal valve region is important as it allows a homogeneous air velocity distribution and laminar flow throughout the nasal cavity<sup>(2,7-9,18,22-25)</sup>. In the normal models, airflow was greatest in the common meatus adjacent to the inferior and middle turbinates but was generally well distributed throughout the nasal cavity. This is consistent with published data<sup>(2,9,22,23)</sup>. Similar to other studies

Table 2. Mean aerodynamic changes of healthy subjects and patients before and after virtual turbinate surgery.

	Healthy (n=2)	Preoperative (n=8)	Turbino-plasty (n=8)	Total inferior turbinectomy (n=8)
Ventilation superior nasal cavity (L/min)	4.1	2.2	1.1	1.1
Ventilation middle nasal cavity (L/min)	3.9	6.2	4.3	4.1
Ventilation inferior nasal cavity (L/min)	7.4	7.1	9.2	10.6
Wall shear stress superior nasal cavity (Pa)	0.018	0.013	0.0094	0.0052
Wall shear stress middle nasal cavity (Pa)	0.067	0.067	0.061	0.038
Wall shear stress inferior nasal cavity (Pa)	0.057	0.060	0.054	0.040
Total pressure drop (Pa)	11	14	9.2	7.9
Average velocity at nasal valve (m/s)	1.2	1.6	1.5	1.5

(7,9,18), it was noted that following any turbinate surgery, the main flow stream was directed inferiorly resulting in less airflow reaching the superior nasal cavity (superior meatus and olfactory cleft). The main flow stream also travelled in a jet-like manner, moving at a higher velocity along a narrower path. Jet-like behaviour was accentuated in the ITR models as the airflow was concentrated in a region adjacent to the inferomedial surface of the middle turbinate, whereas it occupied more space in the inferior meatus in the turbinoplasty group, coming into contact with more of the septum, nasal floor, and lateral wall. The reduction in air-mucosa contact following ITR in these regions has also been reported in the literature (7-9).

This significantly altered flow stream may lead to unfavorable consequences in extremely cold or dry environments. This is because the center of the airstream is likely to remain cool throughout the nasal cavity and although heat exchange occurs adjacent to the mucosa, the overall warming of inspired air is significantly less than that of the normal healthy nose (9). Combined with the disturbed airflow distribution this may have a desiccating effect, causing crusting (9,24,26). Furthermore, the heat and water fluxes needed to condition inspired air may be diminished, adversely impacting alveolar gas exchange, especially in extreme environments (27-29).

Regional ventilation results supported the visual observation of greater airflow in the inferior nasal cavity, accompanied by a

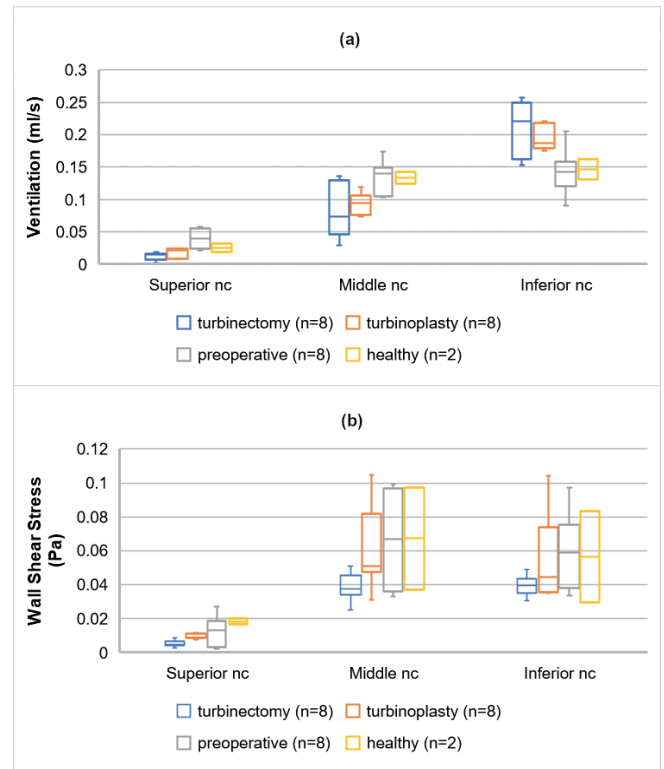


Figure 5. Distribution of ventilation (a) and wall shear stress (b) within superior, middle and inferior nasal cavities; nc = nasal cavity.

trend of reduced airflow in the middle and superior nasal cavity following surgery. Both ventilation and WSS profiles for the turbinoplasty group reflected more closely that of the healthy group. WSS was generally lower for the ITR models compared to the other groups, but this was not consistent for all regions (superior, middle and inferior nasal cavities). Areas of low WSS reflect higher wall temperatures due to reduced mucosal cooling (30). Mucosal cooling where heat fluxes exceed 50W/m<sup>2</sup> has been shown to improve subjective nasal patency scores (12). Following ITR, the surface area receiving heat fluxes that exceed 50 W/m<sup>2</sup> is reduced (7). The simulation of cold receptors may be diminished further by complete turbinate resection, potentially contributing to a paradoxical sensation of nasal obstruction (7,10,12,26). Other physiological consequences of reduced air-mucosa contact may include reduced air warming and humidification (7,12,20,27,31). Nevertheless, given the small differences in WSS between surgery groups, the degree of impact is likely to be negligible unless in extreme environments.

A comparison of pressure variations from the nostril to nasopharynx was made since transnasal pressure drop is proportional to resistance. These were in the range of experimental measurements in cast models, and reported CFD data in the literature (9,21,32). Higher pressures and larger gradients were measured throughout the nasal cavity for the preoperative models compared with the healthy and surgical models. Following turbinate

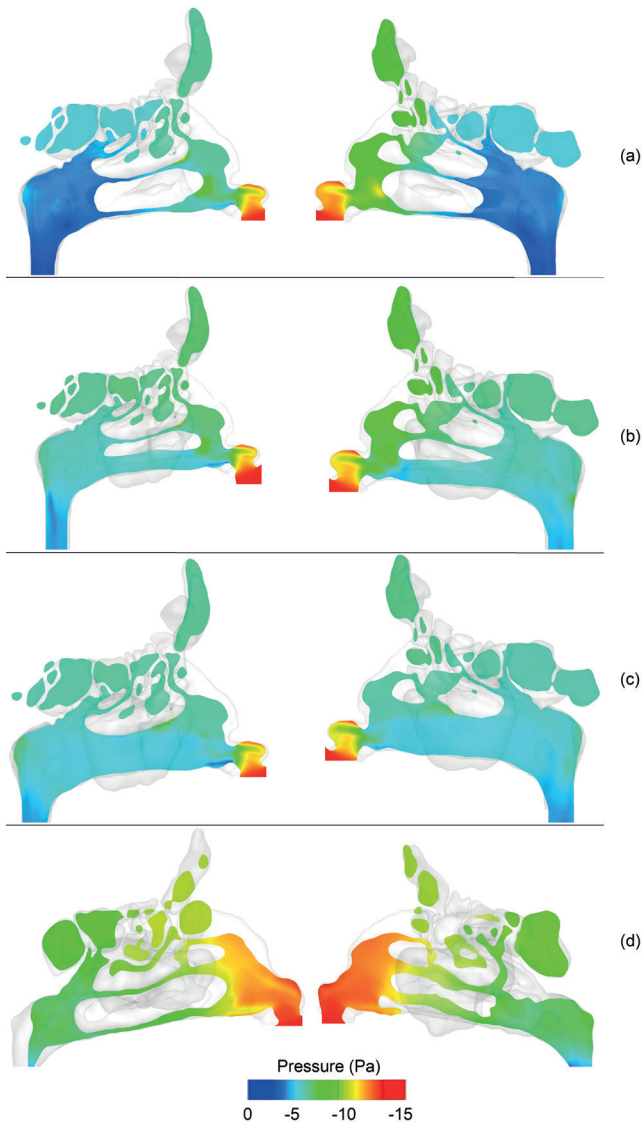


Figure 6. Pressure contours in sagittal view; right sinonasal cavity (left), left sinonasal cavity (right). (a) Preoperative (b) Turbinoplasty (b) Turbinectomy (d) Healthy subject B.

surgery, pressure changes became smoother and smaller as observed in other studies<sup>(9,21)</sup>. There was only a small difference in total transnasal pressure drop between the two surgery groups, which can be mostly attributed to the loss of pressure gradient at the head of the inferior turbinate in the ITR group. The physiological significance of this is uncertain but may relate to normal air conditioning and perception of nasal patency since airflow is a function of pressure gradients. Accordingly, objective tests such as rhinomanometry, peak nasal inspiratory airflow, and acoustic rhinometry use resistance as a measure of patency<sup>(6)</sup>. However, other studies suggests that a change in mucosal temperature correlates better than resistance with nasal patency<sup>(12,13,33-36)</sup>.

Empty nose syndrome (ENS), is a disorder which has received significant clinical research attention<sup>(37,38)</sup>. Our CFD analysis sup-

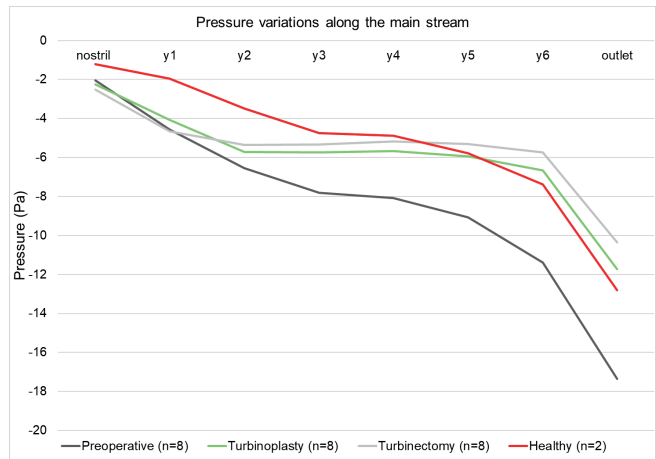


Figure 7. Pressure variation along main airflow stream from nostril to nasopharynx outlet.

ports altered nasal conditioning and characteristics to explain a potential paradoxical obstruction phenomenon following ITR. However, the degree of clinical correlation is unclear, since only a very small subset of patients that undergo radical resection develop long term complications, suggesting that there are additional genetic and environmental factors at play<sup>(39,40)</sup>. ENS remains a controversial topic that deserves further scrutiny with prospective studies that include long term observations.

### Limitations

Although this study has relied on a small number of patients it was able to capture individual variation in nasal geometry, and the extent of surgery performed for a similar clinical condition, as noted by the extent of variation in the volume and surface area reduction following turbino-plasty. Standard inferior turbino-plasty<sup>(4)</sup> has been simulated by the removal of the inferior bulk of turbinate while preserving at least half of its superior portion. The literature describes the simulation of less conventional conservative turbinate reduction methods, suggesting a more minor impact on airflow variables<sup>(9,10,21)</sup>. The present study is a numerical evaluation aiming to characterize the changes and differences in flow dynamics after part or whole of turbinate has been removed. The effect of airflow variables on the clinical condition and subjective perception of surgical outcome remains uncertain. Preoperative objective measurements using PNIF or rhinomanometry would add important insights and these measurements will be included in a follow-on prospective clinical trial that incorporates both objective and subjective measurements with CFD validation.

This CFD study suggests that nasal airflow is significantly altered following turbinate reduction surgery, leading to unique airflow patterns following turbino-plasty and ITR. However, the differences are small, and they should be interpreted carefully until a clinical correlation is established. Future studies should include

long term post-operative clinical data on patients undergoing turbinate surgery to correlate with changes in nasal aerodynamics. However, radical resection of the nasal turbinates is infrequently performed, and symptoms such as recurring nasal obstruction and crusting may take years to develop, thus making such studies difficult.

A rigid wall assumption does not fully replicate the nasal cavity wall. However, the modelling evaluated effects of airway geometry on pressure loss from several locations, and the overall trends in either rigid or flexible walls would remain similar, therefore applying a flexible wall assumption may not yield additional benefit to the aim of the study. Only inspiratory nasal airflow at a restful steady-state was considered as this is the most common breathing state we experience in daily life. Although flow in the nasal cavity is most likely to experience both laminar and turbulent regimes, studies suggest laminar dominant flow behaviour for flows below 20L/min<sup>(41-43)</sup>. For the purposes of engineering and clinical outcomes, the intense and highly demanding computational resources required in unsteady flow modelling may not be justified<sup>(44)</sup>. It is expected that there would be some form of alternating partial congestion and decongestion of each nasal chamber occurring as part of the physiological nasal cycle. Although the extent of this impact on airflow is unknown, variation was considered by including number of patients and using bilateral airway models.

## Conclusions

Total inferior turbinectomy and turbinoplasty significantly alter nasal flow patterns in patients with nasal obstruction caused by inferior turbinate hypertrophy. A slightly greater reduction in nasal airway resistance occurred following turbinectomy which

could be attributed to a significantly smaller pressure gradient at the head of the inferior turbinate. However, turbinoplasty resulted in intra-nasal aerodynamics closer to healthy models. Specifically, a more altered airflow distribution, reduced air-mucosa contact and prominent jet-like course of the main flow stream was observed following turbinectomy. Overall these differences were small and are more likely to bear influence on physiological function in extremely cold and dry environments. On the other hand, since a large proportion of IT mucosa remains following turbinoplasty, it is important to consider future dependence on topical therapy long-term. Further studies using a larger number of patients and healthy subjects are required, attempting to establish a clinical correlation with predicted aerodynamic changes. The overall implication of these changes is that the surgical procedures may need to be carefully planned to minimize the impact on the normal functions of the nose. Future CFD studies can incorporate outcomes such as humidification, warming, and mucociliary clearance in different environments.

## Acknowledgements

This study was supported by a grant from the Garnett Passe and Rodney Williams Memorial Foundation.

## Authorship contribution

All authors have contributed to data collection, data analysis, and the writing of the manuscript.

## Conflict of interest

None

## References

1. Jose J, Coatesworth AP. Inferior turbinate surgery for nasal obstruction in allergic rhinitis after failed medical treatment. *Cochrane Database of Systematic Reviews* 2010
2. Tan J, Han D, Wang J, Liu T, Wang T, Zang H, et al. Numerical simulation of normal nasal cavity airflow in Chinese adult: a computational flow dynamics model. *Eur Arch Otorhinolaryngol* 2012;269:881-9
3. Aldren C, Toley NS. Further studies on nasal sensation of airflow. *Rhinology* 1991;29:59-5
4. Passali D, Anselmi M, Lauriello M, Bellussi L. Treatment of Hypertrophy of the Inferior Turbinate: Long-Term Results in 382 Patients Randomly Assigned to Therapy. *Ann Otol, Rhinol Laryngol* 1999;108:569-75
5. Batra PS, Seiden AM, Smith TL. Surgical management of adult inferior turbinate hypertrophy. *Laryngoscope* 2009;119:1819-27
6. André RF, Vuyk HD, Ahmed A, Graamans K, Nolst Trenité GJ. Correlation between subjective and objective evaluation of the nasal airway. A systematic review of the highest level of evidence. *Clin Otolaryngol* 2009;34:518-25
7. Dayal A, Rhee JS, Garcia GJM. Impact of Middle versus Inferior Total Turbinectomy on Nasal Aerodynamics. *Otolaryngol Head Neck Surg* 2016;155:518-25
8. Rhee JS, Pawar SS, Garcia GJ, Kimbell JS. Toward Personalized Nasal Surgery Using Computational Fluid Dynamics. *Arch Facial Plast Surg*. 2011 Sep-Oct;13(5):305-10.
9. B Chen X, C Leong S, Lee H, F H Chong V, Wang DY. Aerodynamic effects of inferior turbinate surgery on nasal airflow - A computational fluid dynamics model. *Rhinology*. 2010 Dec;48(4):394-400.
10. Na Y, Soo Chung K, Chung S-K, Kim SK. Effects of single-sided inferior turbinectomy on nasal function and airflow characteristics. *Respir Physiol Neurobiol*. 2012;180(2-3):289-97.
11. Patel RG, Garcia GJ, Frank-Ito DO, Kimbell JS, S RJ. Simulating the nasal cycle with computational fluid dynamics. *Otolaryngol Head Neck Surg* 2015;152:353-60
12. Sullivan CD, Garcia GJM, Frank-Ito DO, Kimbell JS, Rhee JS. Perception of Better Nasal Patency Correlates with Increased Mucosal Cooling after Surgery for Nasal Obstruction. *Otolaryngol Head Neck Surg* 2013;150:139-47.
13. Sozansky J, Houser SM. The physiological mechanism for sensing nasal airflow: A literature review. *Int Forum Allergy Rhinol*. 2014;4:834-8
14. Li C, A Farag A, Leach J, Deshpande B, Jacobowitz A, Kim K, et al. Computational Fluid Dynamics and Trigeminal Sensory Examinations of Empty Nose Syndrome Patients. *Laryngoscope*. 2017 Jun;127(6):E176-E184.
15. Siu J, Johnston JJ, Pontre B, Inthavong K, Douglas RG. Magnetic resonance imaging evaluation of the distribution of spray and irrigation devices within the sinonasal cavities. *Int Forum Allergy Rhinol*. 2019;9:958-70
16. Inthavong K, Chetty A, Shang Y, Tu J.

- Examining mesh independence for flow dynamics in the human nasal cavity. *Comput Biol Med.* 2018;102:40-50
17. Lindemann J, Keck T, Wiesmiller KM, Rettinger G, Brambs H-J, Pless D. Numerical simulation of intranasal air flow and temperature after resection of the turbinates. *Rhinology* 2005;43:24-8
  18. Meng-Yang D, Zhe J, Zhi-Qiang G, Zhi L, Yi-Ran A, Wei L. Numerical simulation of airflow fields in two typical nasal structures of empty nose syndrome: a computational fluid dynamics study. *PLoS ONE* 2013;8:e84243
  19. Ozlugedik S, Nakiboglu G, Sert C, Elhan A, Tonuk E, Akyar S, et al. Numerical Study of the Aerodynamic Effects of Septoplasty and Partial Lateral Turbinectomy. *Laryngoscope* 2008;118:330-4
  20. Tsakiropoulou E, Vital V, Constantinidis J, Kekes G. Nasal Air-Conditioning after Partial Turbinectomy: Myths versus Facts. *Am J Rhinol Allergy* 2015;29:e59-e62
  21. Wexler D, Segal R, Kimbell J. Aerodynamic effects of inferior turbinate reduction: computational fluid dynamics simulation. *Arch Otolaryngol Head Neck Surg* 2005;131:1102
  22. Wen J, Inthavong K, Tu J, Wang S. Numerical simulations for detailed airflow dynamics in a human nasal cavity. *Respir Physiol Neurobiol* 2008 161:125-35
  23. Zhao K, Jiang J. What is normal nasal airflow? A computational study of 22 healthy adults. *Int Forum Allergy Rhinol* 2014;4:435-46
  24. Grützmacher S, Lang C, Mlynski G. The Combination of Acoustic Rhinometry, Rhinoresistometry and Flow Simulation in Noses before and after Turbinate Surgery: A Model Study. *ORL* 2003;65:341-7
  25. Dayal P, Shaik MS, Singh M. Evaluation of different parameters that affect droplet-size distribution from nasal sprays using the Malvern Spraytec. *J Pharm Sci* 2004;93:1725-42
  26. Moore EJ, Kern EB. Atrophic Rhinitis: A Review of 242 Cases. *Am J Rhinol.* 2001;15:355-61
  27. Naftali S, Rosenfeld M, M W, Elad D. The air-conditioning capacity of the human nose. *Ann Biomed Eng* 2005;33:545-53
  28. Hyrkäs-Palmu H, Ikäheimo TM, Laatikainen T, Jousilahti P, Jaakkola MS, Jaakkola JJK. Cold weather increases respiratory symptoms and functional disability especially among patients with asthma and allergic rhinitis. *Sci Rep* 2018;8:10131
  29. D'Amato M, Molino A, Calabrese G, Cecchi L, Annesi-Maesano I, D'Amato G. The impact of cold on the respiratory tract and its consequences to respiratory health. *Clin Transl Allergy.* 2018;8:20
  30. Elad D, Naftali S, Rosenfeld M, Wolf M. Physical stresses at the air-wall interface of the human nasal cavity during breathing. *J Appl Physiol.* 2006;100:1003-10
  31. Schroter RC, Watkins NV. Respiratory heat exchange in mammals. *Resp Physiol* 1989;78:357-67
  32. Weinhold I, Mlynski G. Numerical simulation of airflow in the human nose. *Eur Arch Otorhinolaryngol* 2004;261:452-5
  33. Clarke RW, Jones AS, Charters P, Sherman I. The role of mucosal receptors in the nasal sensation of airflow. *Clin Otolaryngol All Sci* 1992;17:383-7
  34. Burrow A, Eccles R, Jones AS. The Effects of Camphor, Eucalyptus and Menthol Vapour on Nasal Resistance to Airflow and Nasal Sensation. *Acta Oto-Laryngologica* 1983;96:157-61
  35. Eccles R, Morris S, Tolley NS. The effects of nasal anaesthesia upon nasal sensation of airflow. *Acta Oto-Laryngol* 1988;106:152-5
  36. Meusel T, Negoias S, Scheibe M, Hummel T. Topographical differences in distribution and responsiveness of trigeminal sensitivity within the human nasal mucosa. *Pain* 2010;151:516-21
  37. Payne SC. Empty nose syndrome: what are we really talking about? *Otolaryngol Clin North Am.* 2009;42:331-7, ix-x
  38. Gill AS, Said M, Tollefson TT, Steele TO. Update on empty nose syndrome: disease mechanisms, diagnostic tools, and treatment strategies. *Curr Opin Otolaryngol Head Neck Surg.* 2019;27:237-42
  39. Eliashar R. Total inferior turbinatectomy: operative results and technique. *Ann Otol Rhinol Laryngol.* 2001;110:700
  40. Talmon Y, Samet A, Gilbey P. Total inferior turbinatectomy: operative results and technique. *Ann Otol Rhinol Laryngol.* 2000;109:1117-9
  41. Doorly DJ, Taylor DJ, Schroter RC. Mechanics of airflow in the human nasal airways. *Respir Physiol Neurobiol* 2008;163:100-10
  42. Li C, Jiang J, Dong H, Zhao K. Computational modeling and validation of human nasal airflow under various breathing conditions. *J Biomech* 2017;64:59-68
  43. Hahn I, Scherer PW, Mozell MM. Velocity profiles measured for airflow through a large-scale model of the human nasal cavity. *J Appl Physiol.* 1993;75:2273-87
  44. Inthavong K, Tian ZF, Li HF, Tu JY, Yang W, Xue CL, et al. A Numerical Study of Spray Particle Deposition in a Human Nasal Cavity. *Aerosol Sci Technol.* 2006;40:1034-45

**Prof Richard Douglas**  
 Department of Surgery  
 The University of Auckland  
 Private Bag 92019  
 Auckland 1142  
 New Zealand

**Tel: +64 9 923 9820**

**Fax: +64 9 377 9656**

**E-mail:**

**richard.douglas@auckland.ac.nz**